Nonlinear Analysis: Modelling and Control, Vol. 23, No. 3, 437–456 ISSN 1392-5113
https://doi.org/10.15388/NA.2018.3.9

Modelling the enzyme catalysed substrate conversion in a microbioreactor acting in continuous flow mode*

Romas Baronas[a], **Juozas Kulys**[b], **Linas Petkevičius**[a,1]

[a]Institute of Computer Science, Vilnius University,
Didlaukio str. 47, LT-08303 Vilnius, Lithuania
linas.petkevicius@mif.vu.lt

[b]Institute of Biochemistry, Life Sciences Center, Vilnius University,
Saulėtekio ave. 7, LT-10257 Vilnius, Lithuania

Received: December 8, 2017 / **Revised:** March 18, 2018 / **Published online:** April 20, 2018

Abstract. A model for the numerical simulation of the action of microbioreactor acting in the continuous flow mode was developed. The microbioreactor system was mathematically modelled by a two-compartment model based on transient reaction-diffusion equations containing a non-linear term related to the Michaelis–Menten kinetics of the enzymatic reaction. The effectiveness of microbioreactor and the process duration were numerically and partially analytically analysed at transition and steady-state conditions in a wide range of model parameters. The computational simulation was carried out using the finite difference technique. The performed calculations showed nonlinear effects of the internal and external diffusion limitations on the effectiveness and process duration.

Keywords: modelling, diffusion-reaction, microreactor, enzyme kinetics, effectiveness factor.

1 Introduction

Bioactive materials like enzymes as process catalysts have been widely used in chemical, environmental, food and pharmaceutical industries [20, 40, 45]. Immobilized enzymes have been recently preferred over dissolved enzymes in stirred reactor systems [26]. Stirred tank bioreactors have been widely used since they favour a good distribution of substrate over the enzyme [27]. When immobilized enzyme is attached to an impermeable solid support, the substrate is carried to the active sites of catalyst through the external diffusion layer. However, the enzyme is rather often entrapped within a porous ceramic or silica particles [2, 7]. In such cases, the substrate must also diffuse through the porous media to reach the enzyme [20]. Thus, the intraparticle diffusion resistance should be considered in conjugation with the external mass transfer resistance.

*This research was supported by a grant (No. S-MIP-17-98) from the Research Council of Lithuania.
[1]Corresponding author.

The problem to measure key physical and biochemical parameters is among the main drawbacks in biotechnological process control [20,26,45]. Multiple physical experiments is one way to identify and improve characteristics of the microreactor. Another way is to model and simulate the processes within microreactors using state-of-the-art techniques of computational modelling [4].

Mathematical models act as an important tool in various bioreactor applications including protein synthesis and bioethanol production [16, 25, 38]. These models are useful for planning efficient process control strategies and predicting the production performance. The simulation approach allows to optimize the microreactor configuration with substantially reduced time and cost [6, 35].

When modelling microbioreactors where the intraparticle and external diffusion resistance is considered, multi-compartment models are required to achieve a sufficient accuracy of the model [8, 41, 44]. Nevertheless, mono compartment models, in which the internal mass transport by diffusion and substrate conversion is considered, are still used in different applications due to the model simplicity [6,7]. Furthermore, the substrate conversion is often studied only in the case were the enzyme kinetics approaches either first or zero-order kinetics [20, 30, 38].

The external diffusion is usually modelled by mass flux boundary condition involving the mass transfer rate of the boundary layer in the presence of diffusive and convective flows [1, 16, 34]. Adequate mass transfer is required in order to successfully model bioprocess experiments [40]. However, the mass transfer coefficient can only be estimated on the basis of rather sophisticated measurements [38].

The goal of this work was to investigate in detail the influence of the physical and kinetic parameters on the effectiveness of the bioreactor system based on a porous spherical mircrobioreactor acting in the continuous flow mode. The microreactor system was mathematically modelled by a two-compartment model based on transient reaction-diffusion equations containing a nonlinear term related to the Michaelis–Menten kinetics of the enzymatic reaction [4, 41]. As the external diffusion was modelled by a diffusion shell surrounding the microreactor, the mathematical model explicitly includes no mass transfer rate.

The effectiveness of the microbioreactor and the process duration were numerically and partially analytically analysed at transition and steady-state conditions in a wide range of model parameters. The computational simulation was carried out using the finite difference technique [15]. The performed calculations showed nonlinear effects of the internal and external diffusion limitations on the microreactor effectiveness and process duration. Particularly, it was determined that increasing the effectiveness by decreasing the internal diffusion limitation is restricted when a short processing time is of crucial importance.

2 Mathematical model

We consider a porous spherical microreactor (MR) placed in a buffer solution containing a substrate. The model of the bioreactor system involves three regions: an enzyme-loaded

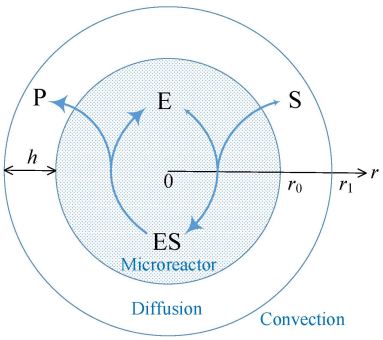

Figure 1. Schematic view of the cross section of a modelled unit cell: biocatalytic microreactor and surrounding shell.

porous microparticle (microreactor), where the enzymatic reaction as well as the mass transport by diffusion take place, a diffusion limiting shell, where only the diffusion takes place, and a convective region, where the substrate concentration remains constant due to continuous flow.

In the enzyme-loaded MR, we consider the enzyme-catalyzed reaction

$$\mathrm{S} \xrightarrow{\mathrm{E}} \mathrm{P}, \tag{1}$$

where the substrate (S) binds to the enzyme (E) and is converted to the product (P) [18, 20]. The principal structure of the unit cell is presented in Fig. 1.

At the quasi-steady-state conditions, the kinetics of most enzyme reactions, including reaction (1), are reasonably well represented by the Michaelis–Menten equation

$$v(s) = \frac{v_{\max} s}{k_M + s},$$

where v is the volumetric reaction rate expressed as a function of the substrate concentration s, $v_{\max}$ is the maximal enzymatic rate, and k_M is the Michaelis constant [20,41,45].

2.1 Governing equations

The dynamics of the MR system includes changes over time of the substrate consumption as well as the product production. Since the reaction product is produced at the same rate as the substrate is consumed, the dynamics of the MR operation can be qualitatively expressed by dynamics only of the substrate concentration [12, 20]. Assuming the symmetrical geometry of the spherical MR and homogenized distribution of the immobilized enzyme inside the MR, the mathematical model can be described in one-dimensional domain using the radial distance ($0 < r < r_0$, $t > 0$),

$$\frac{\partial s_m}{\partial t} = d_m \Delta s_m - v(s_m), \tag{2}$$

where $s_m = s_m(r,t)$ is the concentration of the substrate in the MR, Δ is the Laplace operator, r_0 is the radius of the MR, d_m is the effective diffusion coefficient [11, 41].

Assuming the solution is permanently stirred and applying the Nernst approach, a thin spherical shell (the Nernst diffusion layer) adjacent to the MR surface remains stagnant with time ($r_0 < r < r_1, t > 0$),

$$\frac{\partial s_d}{\partial t} = d_d \Delta s_d, \tag{3}$$

where $s_d = s_d(r,t)$ is the concentration of the substrate in the diffusion shell, d_d is the corresponding diffusion coefficient, and $h = r_1 - r_0$ is the thickness of the spherical diffusion shell [11, 15, 45].

2.2 Initial and boundary conditions

It was assumed that, initially ($t = 0$), the MR is uniformly loaded with the enzyme and is free of the substrate,

$$s_m(r,0) = 0, \quad 0 \leqslant r \leqslant r_0. \tag{4}$$

The reaction starts when the MR is poured into the container containing some substrate distributed uniformly outside the MR,

$$s_d(r,0) = s_0, \quad r_0 \leqslant r \leqslant r_1, \tag{5}$$

where s_0 is the substrate concentration in the bulk.

Due to the symmetry, the zero-flux boundary condition is defined for the centre of the spherical microreactor ($t > 0$),

$$d_m \frac{\partial s_m}{\partial r}\bigg|_{r=0} = 0. \tag{6}$$

Away from the diffusion shell ($r > r_1$), the solution is uniform throughout the outside of the shell and remains constant ($t > 0$) [19],

$$s_d(r_1,t) = s_0. \tag{7}$$

The formal partition coefficient ϕ is used in the matching conditions to describe the specificity in the concentration distribution of the substrate between two neighboring regions ($t > 0$),

$$d_m \frac{\partial s_m}{\partial r}\bigg|_{r=r_0} = d_d \frac{\partial s_d}{\partial r}\bigg|_{r=r_0}, \tag{8}$$

$$s_m(r_0,t) = \phi s_d(r_0,t). \tag{9}$$

The partition coefficient ϕ is less than unity as the averaged concentration of the substrate in the MR becomes less than the concentration in the bulk solution due to the insoluble MR carrier [17, 44].

We assume that the system approaches a steady-state as $t \to \infty$,

$$s_{m,s}(r) = \lim_{t\to\infty} s_m(r,t), \qquad s_{d,s}(r) = \lim_{t\to\infty} s_d(r,t).$$

2.3 Dimensionless model

In order to reduce the number of model parameters, a dimensionless model was derived by introducing the following dimensionless variables [44]:

$$R=\frac{r}{r_0},\qquad R_1=\frac{r_1}{r_0},\qquad H=\frac{r_1-r_0}{r_0},\qquad T=\frac{d_m t}{r_0^2},\qquad \theta=\frac{d_d}{d_m},$$
$$S_m=\frac{s_m}{k_M},\qquad S_d=\frac{s_d}{k_M},\qquad S_0=\frac{s_0}{k_M},\qquad S_{m,s}=\frac{s_{m,s}}{k_M},\qquad S_{d,s}=\frac{s_{d,s}}{k_M}.$$

The governing equations (2) and (3) in the dimensionless form are then expressed as follows ($T>0$):

$$\begin{aligned}\frac{\partial S_m}{\partial T}&=\Delta S_m-\sigma^2\frac{S_m}{1+S_m},\quad R\in(0,1),\\ \frac{\partial S_d}{\partial T}&=\theta\Delta S_d,\quad R\in(1,R_1),\end{aligned}\tag{10}$$

where dimensionless factor σ^2 is known as the dimensionless diffusion module or the Damköhler number or Thiele modulus [22, 31, 41],

$$\sigma^2=\frac{v_{\max}r_0^2}{k_M d_m}.\tag{11}$$

The initial conditions (4) and (5) are transformed to the following conditions:

$$\begin{aligned}S_m(R,0)&=0,\quad R\in[0,1],\\ S_d(R,0)&=S_0,\quad R\in[1,\,R_1].\end{aligned}\tag{12}$$

The boundary conditions (6)–(9) are rewritten as follows ($T>0$):

$$\begin{aligned}\left.\frac{\partial S_m}{\partial R}\right|_{R=0}&=0,\qquad S_d(R_1,T)=S_0,\\ \left.\frac{\partial S_m}{\partial R}\right|_{R=1}&=\theta\left.\frac{\partial S_d}{\partial R}\right|_{R=1},\qquad S_m(1,T)=\phi S_d(1,T).\end{aligned}\tag{13}$$

3 Characteristics of microbioreactor action

The effectiveness factors characterise the interaction between diffusion and reactions in porous catalytic pellets, microreactors and solid fuel particles [12, 19]. Reactants have to diffuse through the external diffusion layer and pores of the support for the reaction to take place, and therefore, the actual rate can be limited by the rate at which the diffusing reactants reach the catalyst. Typically designers seek for bioreactors acting in the reaction-limited regime since, in this case, reaction and diffusion occur on different time scales and one is in the best possible position to measure reaction [21].

Since the effectiveness of a bioreactor can be defined with respect to the concentration at the catalyst surface or with respect to the bulk concentration, the internal and external effectiveness factors are often used in the biochemical engineering [19, 20]. Additionally, the effectiveness factor due to partitioning is also used when taking into consideration the partitioning effect [46].

The effectiveness factors are usually defined for the stationary mode of biocatalytic systems [12, 20, 23]. An analysis of the transient effectiveness factors, in opposition to the conventional steady-state approach, is recommended only in the cases where strong adsorption of reactant molecules, previous to surface reaction, exists [13]. On the other hand, although the transient effectiveness factors in porous catalyst particles can be considered [13], after very short time, the substrate concentration inside the particles becomes constant, and the effectiveness of reactor system in the beginning of the process is not important for overall effectiveness of the system acting in the flow mode [20].

The internal effectiveness factor η_i for the MR can be defined as the ratio of the actual volume-averaged rate of the reaction over the whole MR to the rate of the reaction at the inner surface of the MR [11, 18, 20],

$$\eta_i = \frac{(4\pi \int_0^{r_0} v(s_{m,s}(r))r^2 \,\mathrm{d}r)/(4\pi r_0^3/3)}{v(s_{m,s}(r_0))} = \frac{3\int_0^{r_0} v(s_{m,s}(r))r^2 \,\mathrm{d}r}{r_0^3 v(s_{m,s}(r_0))}. \tag{14}$$

The factor η_i can be also expressed in terms of the dimensionless model,

$$\eta_i = 3\,\frac{1 + S_{m,s}(1)}{S_{m,s}(1)} \int\limits_0^1 \frac{S_{m,s}(R)}{1 + S_{m,s}(R)} R^2 \,\mathrm{d}R. \tag{15}$$

For η_i near unity, the entire volume of the MR is reacting at the same rate as at the inner surface because the substrate concentration decrease in the MR is insignificant. For η_i near zero, the almost all substrate reacts at the surface of the MR, and the reaction rate decreases in comparison to the rate at the inner surface at the same substrate concentration [20].

The external effectiveness factor η_e is defined as the ratio of the reaction rate that would occur if the substrate concentration over the whole microreactor equal the concentration at the outer surface of the MR to that which would be obtained if the concentration everywhere in the MR equal to the concentration in the bulk [20, 46],

$$\eta_e = \frac{v(s_{d,s}(r_0))}{v(s_0)} = \frac{(1 + S_0)S_{d,s}(1)}{(1 + S_{d,s}(1))S_0}. \tag{16}$$

The external effectiveness factor is a measure of the influence of the external mass transfer resistance on the rate of the observed reaction. If it is significantly less then unity, the mass transfer resistance is restricting the supply of the substrate to the MR surface and is thus limiting the catalytic activity of the enzyme, whereas the reaction is not limited by the external mass transfer if the factor equals unity [20].

The influence of partitioning can be expressed in terms of an effectiveness factor as follows:

$$\eta_p = \frac{v(s_{m,s}(r_0))}{v(s_{d,s}(r_0))} = \frac{(1+S_{d,s}(1))S_{m,s}(1)}{(1+S_{m,s}(1))S_{d,s}(1)}. \tag{17}$$

Taking into consideration the matching conditions (8) and (9), the factor η_p reads

$$\eta_p = \frac{(1+S_{d,s}(1))\phi}{1+\phi S_{d,s}(1)} = \frac{\phi + S_{m,s}(1)}{1+S_{m,s}(1)}. \tag{18}$$

The overall effectiveness factor η_o can be calculated from the internal and external effectiveness factors as well as from the effectiveness factor due to partitioning [46],

$$\eta_o = \eta_i\eta_e\eta_p = 3\,\frac{1+S_0}{S_0}\int\limits_0^1 \frac{S_{m,s}(R)}{1+S_{m,s}(R)}R^2\,\mathrm{d}R. \tag{19}$$

Summarising definitions (14)–(19), the overall (total) effectiveness factor η_o can be defined also as the ratio of the average reaction rate actually observed in the MR to the rate evaluated at the bulk concentrations of the substrate [41, 46].

The process duration is another important characteristic of biotechnological processes [23]. A minimization of time-cost is often sought by designers of biotechnological processes [42]. The holding time t_h and the corresponding dimensionless time T_h required for complete enzymatic conversion of whole amount of the substrate initially added to the reactor system (spherical diffusion shell) were accepted as a measure of time-cost of the bioreactor operation,

$$t_h = \left\{ t\colon \int\limits_0^t \int\limits_0^{r_0} v\big(s_m(r,t)\big)r^2\,\mathrm{d}r\,\mathrm{d}t = \frac{(r_1^3 - r_0^3)s_0}{3} \right\}, \qquad T_h = \frac{d_m t_h}{r_0^2}.$$

4 Solving the model

The nonlinear initial boundary value problem (2)–(9) can be analytically solved only for specific values of the model parameters [4, 20, 41]. Therefore, the problem was solved numerically, using the finite difference technique [15]. In the space direction r, both segments $[0, r_0]$ and $[r_0, r_1]$ were divided into the same number $N = 120$ of small intervals. A uniform discrete grid was also introduced in the time direction t. An explicit finite difference scheme has been built as a result of the difference approximation [15]. Although explicit difference schemes have the strict stability limitations, these schemes have a convenient algorithm of the calculation and are simple for programming [14, 15]. To make the difference scheme stable, the time step size τ was chosen from the sufficient stability condition

$$\tau \leqslant \min\left(\frac{\min\{h_m^2, h_d^2\}}{2\max\{d_m, d_d\}},\ \frac{K_m}{2V_{\max}}\right),$$

where h_m and h_d are step sizes for the MR and diffusion shell, respectively [9]. The simulator has been programmed by the authors in the C++ programming language [36].

In the numerical simulation, the steady-state time t_{ss} was assumed as the time when the normalised change of the substrate concentration remains very small during a relatively long term,

$$t_{ss} = \min_{t>0}\left\{t:\ \frac{t}{s_0}\left|\frac{\mathrm{d}(\frac{3}{r_0^3}\int_0^{r_0} s_m(r,t)r^2\,\mathrm{d}r + \frac{3}{r_1^3-r_0^3}\int_{r_0}^{r_1} s_d(r,t)r^2\,\mathrm{d}r)}{2\mathrm{d}t}\right| < \epsilon\right\},$$

$$s_{m,s}(r) \approx s_m(r,t_{ss}), \quad r\in[0,r_0], \qquad s_{d,s}(r) \approx s_d(r,t_{ss}), \quad r\in[r_0,r_1].$$

In calculations, the decay rate $\epsilon = 10^{-3}$ was used.

The numerical solution of problem (2)–(9) was validated by using exact analytical solutions known for special cases of the model parameters when the nonlinear model approaches its linear counterpart [12, 20, 27, 43]. The relative difference between the analytical and computational steady-state concentrations $s_{m,s}$ and $s_{d,s}$ was less than 1% for different values of the model parameters, $v_{\max}$, h and s_0.

In all the numerical experiments, the following typical values of the model parameters were kept constant [3, 18, 20]:

$$\begin{aligned} d_d &= 600\ \frac{\mu\mathrm{m}^2}{\mathrm{s}}, \qquad d_m = 200\ \frac{\mu\mathrm{m}^2}{\mathrm{s}}, \\ k_M &= 100\ \mu\mathrm{M}, \qquad r_0 = 250\ \mu\mathrm{m}, \qquad \phi = 0.6. \end{aligned} \tag{20}$$

Figure 2 shows the dynamics of the substrate concentration calculated for moderate concentration of the substrate ($s_0 = k_M$, $S_0 = 1$), the diffusion shell thickness h of 60 μm and the following two values of the maximal enzymatic rate $v_{\max}$: 1 and 10 μM/s.

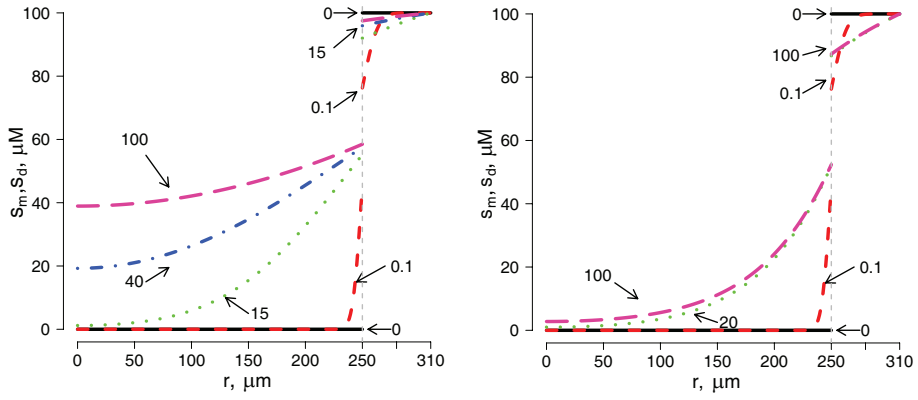

Figure 2. Profiles of the substrate concentration at different time (t) points calculated at $s_0 = 100$ μM, $h = 60$ μm and two values of $v_{\max}$: 1 (a) and 10 (b) μM/s. The other parameters are as defined in (20). Numbers on arrows indicate time in seconds.

Applying the model parameter values defined in (20), the maximal enzymatic rates $v_{\max} = 1\mu\mathrm{M/s}$ (Fig. 2(a)) and $v_{\max} = 10\mu\mathrm{M/s}$ (Fig. 2(b)) correspond to the following two approximate values of the diffusion module σ: 1.8 and 5.6. Since the substrate concentration (s_0 and S_0) and the Biot number $\beta = 15.5$ were the same in both numerical experiments, Fig. 2 illustrates mainly the effect of the diffusion module σ on the concentration within the MR as well as on the effectiveness of the MR.

For model parameter values $S_0 = 1$, $\beta = 15.5$ and $\sigma = 1.8$ (Fig. 2(a)) used in the simulations, the calculated effectiveness factors are as follows: $\eta_i = 0.92$, $\eta_e = 0.99$, $\eta_p = 0.75$, $\eta_o = 0.68$, while at greater value of $\sigma = 5.6$ (Fig. 2(b)): $\eta_i = 0.55$, $\eta_e = 0.93$, $\eta_p = 0.74$, $\eta_o = 0.38$, i.e. the greater value of σ corresponds to lower effectiveness of the MR. On the other hand, the numerical experiments showed that increasing in the diffusion module σ leads to decreasing the holding time, $T_h = 0.85$ ($t_h = 266$ s) at $\sigma = 1.8$ and $T_h = 0.146$ ($t_h = 45$ s) at $\sigma = 5.6$. Below, these effects are investigated in details.

In most numerical experiments carried out in this work, the holding time t_h was significantly greater than the steady-state time t_{ss}. When the steady-state is reached, the substrate concentration $s_m(r,t)$ as well as the enzyme reaction rate $v(s_m(r,t))$ stays unchanged with time, $v(s_m(r,t)) = v(s_{m,s}(r))$ for $t > t_{ss}$. Because of this, the time t_h can be rather precisely evaluated from the concentrations calculated until steady-state is reached only if $t_h > t_{ss}$,

$$t_h \approx \left\{ t\colon \int_0^{t_{ss}} \int_0^{r_0} v\big(s_m(r,t)\big) r^2 \,\mathrm{d}r \,\mathrm{d}t + (t - t_{ss}) \int_0^{r_0} v\big(s_{m,s}(r)\big) r^2 \,\mathrm{d}r = \frac{(r_1^3 - r_0^3) s_0}{3} \right\}$$

$$= t_{ss} + \left(\frac{(r_1^3 - r_0^3) s_0}{3} - \int_0^{t_{ss}} \int_0^{r_0} v\big(s_m(r,t)\big) r^2 \,\mathrm{d}r \,\mathrm{d}t \right) \Big/ \int_0^{r_0} v\big(s_{m,s}(r)\big) r^2 \,\mathrm{d}r.$$

4.1 First-order steady-state solution

At low concentration of the substrate ($s_0 \ll k_M$), the Michaelis–Menten kinetics approaches the first-order kinetics, $v(s_m) \approx v_{\max} s_m / k_M$. Then, assuming the steady-state approximation, the governing equations (2) and (3) reduce to the following equations:

$$d_m \frac{\partial}{\partial r}\left(r^2 \frac{\partial s_{m,s}}{\partial r} \right) = \frac{v_{\max} s_{m,s}}{k_M} r^2, \qquad \frac{\partial}{\partial r}\left(r^2 \frac{\partial s_{d,s}}{\partial r} \right) = 0. \tag{21}$$

The linear boundary value problem (21), (6)–(9) can be easily solved [12],

$$s_{m,s}(r) = \frac{\phi s_0 r_1}{r} \frac{\theta r_0 \sinh \frac{\sigma r}{r_0}}{\theta r_1 \sinh\sigma + \phi(r_1 - r_0)(\sigma\cosh\sigma - \sinh\sigma)}, \quad 0 \leqslant r \leqslant r_0, \tag{22}$$

$$s_{d,s}(r) = \frac{s_0 r_1}{r} \frac{\theta r \sinh\sigma + \phi(r - r_0)(\sigma\cosh\sigma - \sinh\sigma)}{\theta r_1 \sinh\sigma + \phi(r_1 - r_0)(\sigma\cosh\sigma - \sinh\sigma)}, \quad r_0 \leqslant r \leqslant r_1. \tag{23}$$

Analytical expressions (22)–(23), obtained for the substrate concentration at the steady-state, can be applied to evaluating the effectiveness factors,

$$\eta_i = \frac{3}{\sigma^2}(\sigma \coth \sigma - 1), \tag{24}$$

$$\eta_e = \frac{\beta}{\beta + \phi(\sigma \coth \sigma - 1)}, \tag{25}$$

$$\eta_p = \phi,$$

$$\eta_o = \frac{3\beta\phi(\sigma \coth \sigma - 1)}{\sigma^2(\beta + \phi(\sigma \coth \sigma - 1))}, \tag{26}$$

where

$$\beta = \frac{\theta r_1}{r_1 - r_0} = \frac{d_d r_1}{d_m(r_1 - r_0)} = \frac{d_d(r_0 + h)}{d_m h}. \tag{27}$$

The dimensionless factor β can be considered as the effective Biot number or dimensionless mass transfer coefficient that quantifies the relative preponderance of internal or external diffusion [4]. Expression (27) of the Biot number β was deduced by substituting expressions (22) and (23) into the boundary condition (8) and rewriting it in the dimensionless form as the flux condition [33],

$$\left.\frac{\partial S_{m,s}}{\partial R}\right|_{R=1} = \beta\big(1 - S_{d,s}(1)\big).$$

The Biot number is usually defined as a function of the mass transfer coefficient, characteristic length and mass diffusivity [4]. The mass transfer coefficient is dependent on the system geometry, the physical properties of medium and flow dynamics, and it is hard to evaluate the mass transfer resistance between biocatalytic reactors and liquids [3, 18,38]. That is why the effectiveness factors are sometimes estimated without the external mass transfer resistance [34, 46]. The Biot number β defined in (27) depends only on the geometry of the diffusion shell and diffusivity of the substrate.

A low Biot number means the strong external mass transfer resistance, and hence, both internal and external mass transfer resistances are important for the determination of substrate conversion. As the Biot number increases, the importance of the external mass transfer resistance decreases [1]. Since $r_0 \leqslant r_1$, the effective Biot number β ranges from $\theta = d_d/d_m$ ($r_1 \gg r_0$, $h \gg r_0$) to ∞ ($r_1 \to r_0$, $h \to 0$), and since $d_m \leqslant d_d$, the Biot number $\beta \geqslant 1$ [46]. As the thickness h of the external diffusion shell depends upon the nature and intensity of the stirring of the buffer solution, the less intense stirring corresponds to lower β (greater h), and more intense stirring corresponds to greater β (lower h). The diffusion module and the Biot number are widely used in analysis and design of different bioreactors [16, 30, 43].

Expression (24) of the internal effectiveness factor is invariant to the external mass transfer and is equivalent to another already known expression defined in terms of the Thiele modulus [20, 27, 43]. The dependence of the external effectiveness factor only

on the diffusion module and Biot number defined through the external mass transfer coefficient is also known [3]. Expression (25) of the external effectiveness factor η_e involves the Biot number β defined through the diffusion coefficients and the geometry of the diffusion shell.

Both internal and external effectiveness factors are monotonous decreasing functions of the diffusion module σ, $\eta_i \to 0$ and $\eta_e \to 0$ as $\sigma \to \infty$, and $\eta_i \to 1$ and $\eta_e \to 1$ as $\sigma \to 0$. In addition, the external effectiveness factor is an increasing function of the Biot number, $\eta_e \to 1$ as $\beta \to \infty$, and $\eta_e \to 0$ as $\beta \to 1$. Since β decreases with increasing the thickness $h = r_1 - r_0$ of the external diffusion layer, the external effectiveness factor η_e monotonously decreases with increasing the thickness h.

After introducing the Biot number β, expression (22) of the substrate concentration inside the MR reduces as follows:

$$s_{m,s}(r) = \frac{\phi s_0}{r} \frac{\beta r_0 \sinh \frac{\sigma r}{r_0}}{\beta \sinh \sigma + \phi(\sigma \cosh \sigma - \sinh \sigma)}, \quad 0 \leqslant r \leqslant r_0. \tag{28}$$

Accordingly, the dimensionless substrate concentration $S_{m,s}$ depends on the dimensionless concentration S_0, diffusion module σ, Biot number β, partition coefficient ϕ and space coordinate R, and $S_{d,s}$ additionally depends on the dimensionless radius R_1,

$$S_{m,s}(R) = \frac{\phi S_0}{R} \frac{\beta \sinh(\sigma R)}{\beta \sinh \sigma + \phi(\sigma \cosh \sigma - \sinh \sigma)}, \quad 0 \leqslant R \leqslant 1,$$

$$S_{d,s}(R) = \frac{S_0}{R} \frac{\beta R \sinh \sigma + \phi R_1(\sigma \cosh \sigma - \sinh \sigma)\frac{R-1}{R_1-1}}{\beta \sinh \sigma + \phi(\sigma \cosh \sigma - \sinh \sigma)}, \quad 1 \leqslant R \leqslant R_1.$$

When the external mass transfer by diffusion is ignored ($h \to 0$, $\beta \to \infty$), expressions (22) and (28) reduce to a known formulae [12, 20, 27, 43].

4.2 Zero-order steady-state solution

At high concentration of the substrate ($s_0 \gg k_M$), the Michaelis–Menten kinetics approaches the zero-order kinetics, $v(s_m) \approx v_{\max}$. At the steady-state, the governing equations (2) and (3) reduce to the following system:

$$d_m \frac{\partial}{\partial r}\left(r^2 \frac{\partial s_{m,s}}{\partial r}\right) = v_{\max} r^2, \qquad \frac{\partial}{\partial r}\left(r^2 \frac{\partial s_{d,s}}{\partial r}\right) = 0. \tag{29}$$

Solving boundary value problem (29), (6)–(9) gives the following expressions:

$$s_{m,s}(r) = \phi s_0 - \frac{v_{\max}}{6d_m}\left(r_0^2 - r^2 + \frac{2\phi r_0^2}{\beta}\right), \quad 0 \leqslant r \leqslant r_0, \tag{30}$$

$$s_{d,s}(r) = s_0 - \frac{v_{\max} r_0^3}{3d_d}\left(\frac{1}{r} - \frac{1}{r_1}\right), \quad r_0 \leqslant r \leqslant r_1.$$

Since the reaction rate in the governing equation (29) is independent of the substrate concentration, its solution can produce a negative concentration of the substrate. The maximal MR radius r_0, for which expression (30) can be used, is

$$r_{\max} = \sqrt{\frac{6d_m\phi s_0}{v_{\max}(1+\frac{2\phi}{\beta})}}.$$

Since in the case of zero-order reactions the reaction rate is independent of the substrate concentration, the effectiveness factors approaches their maximal values, $\eta_i = \eta_e = \eta_p = 1$, $\eta_o = 1$, if only $r_0 \leqslant r_{\max}$.

The derived expression (30) generalises a known expression of the substrate concentration inside the spherical bioreactor when the external mass transfer is ignored and $r_0^2 \leqslant 6d_m\phi s_0/v_{\max}$ [20].

4.3 Nonlinear steady-state solution

Over the last two decades, some nonlinear reaction-diffusion equations have been analytically solved by applying the homotopy perturbation method (HPM) [24]. This method, which is a combination of homotopy in topology and classic perturbation techniques, provides a convenient way to obtain approximate solutions for a wide variety of problems arising in different fields, including reaction-diffusion equation involving Michaelis–Menten kinetics [29, 39]. However, often accurate analytical solutions obtained by the HPM are not expressed in the closed form and the accuracy of the constructed closed-forms of analytical expressions of the substrate concentration is not satisfactory [37]. Nevertheless, a variety of applications show the usefulness of HPM in solving reaction-diffusion equations [5].

An application of the HPM to the stationary case of the nonlinear reaction-diffusion problem (2)–(9) results in the following approximate analytical expressions of the substrate concentration inside ($s_{m,H}$) and outside ($s_{d,H}$) the MR:

$$\begin{aligned} s_{m,s}(r) &\approx s_{m,H}(r) \\ &= s_0\phi - \frac{P\sigma^2\phi s_0}{2}\left(1 - \frac{r^2}{r_0^2} + \frac{2\phi}{\beta} + \frac{3P^2\sigma^2}{20}\left(8\frac{\phi}{\beta}\left(1+5\frac{\phi}{\beta}\right)\right.\right. \\ &\quad \left.\left. - 3\left(1-\frac{r^4}{r_0^4}\right) + 10\left(1+2\frac{\phi}{\beta}\right)\left(1-\frac{r^2}{r_0^2}\right)\right)\right), \end{aligned} \tag{31}$$

$$\begin{aligned} s_{d,s}(r) &\approx s_{d,H}(r) \\ &= s_0 - \frac{P\sigma^2\phi s_0 r_0}{\theta}\left(\frac{1}{r} - \frac{1}{r_1}\right)\left(1 + \frac{3P^2\sigma^2}{5}\left(1+5\frac{\phi}{\beta}\right)\right), \end{aligned} \tag{32}$$

where $P = k_M/(3(\phi s_0 + k_M)) = 1/(3(\phi S_0 + 1))$.

The substrate concentrations (31) and (32) in the dimensionless form are expressed in a slightly more closed form,

$$\begin{aligned} S_{m,s}(R) &\approx S_{m,H}(R) \\ &= \phi - \frac{P\sigma^2\phi}{2}\left(1 - R^2 + \frac{2\phi}{\beta} + \frac{3P^2\sigma^2}{20}\left(8\frac{\phi}{\beta}\left(1 + 5\frac{\phi}{\beta}\right)\right.\right. \\ &\quad \left.\left. - 3\big(1 - R^4\big) + 10\left(1 + 2\frac{\phi}{\beta}\right)\big(1 - R^2\big)\right)\right), \end{aligned} \tag{33}$$

$$\begin{aligned} S_{d,s}(R) &\approx S_{d,H}(r) \\ &= 1 - \frac{P\sigma^2\phi}{\theta}\left(\frac{1}{R} - \frac{1}{R_1}\right)\left(1 + \frac{3P^2\sigma^2}{5}\left(1 + 5\frac{\phi}{\beta}\right)\right). \end{aligned} \tag{34}$$

Although the form of expressions (31)–(33) is rather complicated, but, nevertheless, their accuracy is not good enough. The expressions of the substrate concentration obtained by HPM are of satisfactory accuracy when the enzyme kinetics controls the MR action, i.e. when $\sigma < 1$, regardless of the Biot number β and the substrate concentration S_0. However, these expressions are practically useless for the systems when the MR acts under diffusion control, especially at low values of β. Nevertheless, since typically designers seek for bioreactors acting in the reaction-limited regime ($\sigma \ll 1$) [21], the expressions of the substrate concentration obtained by HPM have a practical value.

Having the analytical expressions (31)–(33), all the effectiveness factors can be also analytically expressed. However, due to limited use of the substrate expressions and their not closed form, the analytical expressions of the effectiveness factors are not presented in this paper. The numerical solution of the problem is more accurate than the solution obtained by HPM, and because of this, the influence of the model parameter to the effectiveness factors was mainly investigated by numerical simulation of the MR action.

5 Simulation results and discussion

To investigate the effects of the internal and external mass transport by diffusion on the effectiveness of the MR as well as on the duration of the substrate conversion, the MR action was numerically calculated for different values of the model parameters. The overall effectiveness factor η_o was used as the main measure of the MR effectiveness and the dimensionless holding time T_h as a measure of the process duration.

5.1 Impact on effectiveness

To investigate the impact of the diffusion limitations on the MR effectiveness, the factor η_o was numerically calculated for different values of the diffusion module σ, the Biot number β and the dimensionless substrate concentration S_0. Figure 3 shows the factor η_o versus σ and β.

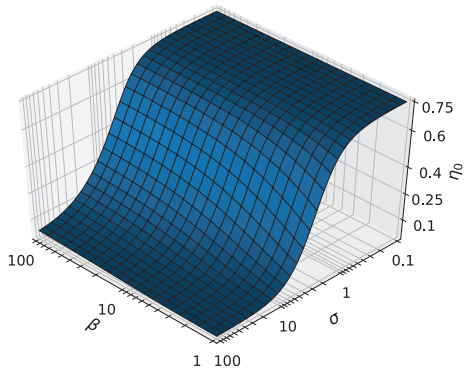

Figure 3. The overall effectiveness factor η_o vs. the diffusion module σ and Biot number β at the dimensionless substrate concentration $S_0 = 1$.

As one can see in Fig. 3, the overall effectiveness factor η_o increases with decreasing the diffusion module σ and approaches to a constant value, which is approximately the same for all values of the Biot number β.

In the case of low substrate concentration ($S_0 \ll 1$) and small values of σ, since $\coth(\sigma) \approx (1/\sigma + \sigma/3)$, according to (26), the factor η_o approaches to ϕ for all possible values of β, i.e. $\eta_o \approx \phi$ for $S_0 \ll 1$ and $\sigma < 1$. Figure 3 shows that η_o approaches the maximum that is slightly higher than ϕ, $\eta_o \to 0.75 > \phi = 0.6$. This is due to not a low substrate concentration ($S_0 = 1$) used in the simulation of the results depicted in Fig. 3. On the other hand, it was already shown that at very high concentrations ($S_0 \gg 1$) of the substrate, the effectiveness factor η_o approaches to unity. Figure 3 also shows that the impact of the Biot number β on the factor η_o is notable only when $\sigma > 1$, i.e. when the MR action is under diffusion control. The effect of β increases with increasing σ.

To determine the influence of the substrate concentration to the effectiveness of MR, the overall effectiveness factor η_o was calculated for very different values of the substrate concentration. Figure 4(a) shows the factor η_o versus the dimensionless concentration S_0 and diffusion module σ at a mean value of the Biot number, $\beta = 10$, and Fig. 4(b) shows η_o versus S_0 and β at a mean value of the diffusion module $\sigma = 1$.

Figures 3 and 4 show that the MR effectiveness can be notably increased by increasing the substrate concentration (S_0) as well as by decreasing the diffusion module σ, i.e. by decreasing the intraparticle diffusion resistance. The effectiveness can be also but slightly increased by increasing the Biot number β, i.e. by decreasing the external diffusion resistance. In the case of low substrate concentration ($S_0 \ll 1$), the fact that η_o is a monotonic increasing function of β can be also noticed from (26).

Figures 3 and 4(a) particularly demonstrate that the MR effectiveness η_o is a monotonic decreasing function of the diffusion module σ and practically stagnates at its maximum value when $\sigma < 1$, i.e. η_o is practically invariant to σ when the enzyme kinetics controls the MR action. Having a MR, which action is controlled by the enzyme kinetics $\sigma < 1$, its effectiveness can not be further increased by decreasing the internal diffusion resistance.

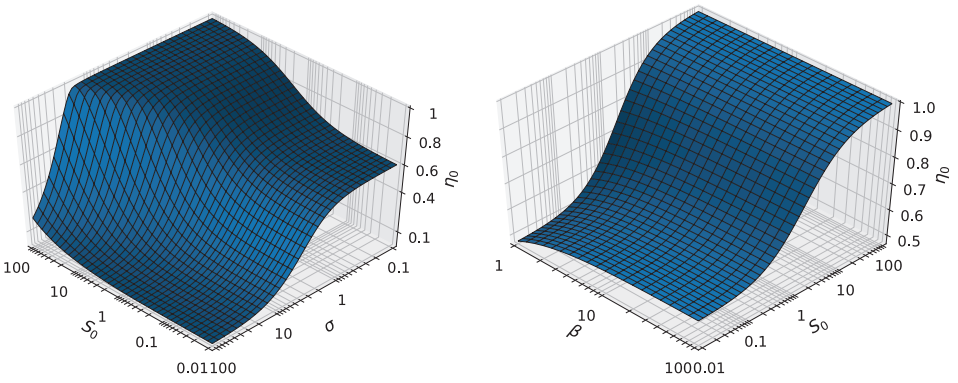

Figure 4. The overall effectiveness factor η_o vs. the dimensionless concentration S_0 changing the diffusion module σ at the Biot number $\beta = 10$ (a) and changing the Biot number β at $\sigma = 1$ (b).

Increasing the internal effectiveness factor η_i with decreasing the diffusion module σ (Thiele module or Damköhler number) has been already reported for the first-order enzyme kinetics ($S_0 \ll 1$) [18, 43]. The dependence of the external effectiveness factor η_e on the Biot number β defined through the external mass transfer coefficient is also already known [3]. Figures 3 and 4 show the overall effectiveness factor versus very wide ranges of three parameters, σ, β and S_0. Figure 4 exclusively shows how the MR effectiveness changes when the enzyme kinetics changes from first-order ($S_0 \ll 1$) through Michaelis–Menten to zero-order ($S_0 \gg 1$) kinetics.

5.2 Impact on process duration

To determine the influence of the diffusion limitations and the initial substrate concentration to the process duration, the MR action was simulated and the dimensionless holding time T_h was calculated by changing values of the diffusion module σ, the Biot number β and the dimensionless substrate concentration S_0. Figure 5 shows calculated values of the time T_h versus σ and β. The dependence of T_h on the substrate concentration is presented in Fig. 6.

As one can see in Fig. 5, the time T_h increases with decreasing both the diffusion module σ and the Biot number β. Figure 5 also shows that the impact of the Biot number β on the time T_h is notable only when $\sigma > 1$, i.e. when the MR action is under diffusion control.

To determine the influence of the substrate concentration to the process duration, the MR action was simulated and the dimensionless time T_h was calculated for very different values of the substrate concentration. Figure 6(a) shows the time T_h versus the dimensionless concentration S_0 and diffusion module σ at a mean value of the Biot number, $\beta = 10$, and Fig. 4(b) shows T_h versus S_0 and β at a mean value of the diffusion module $\sigma = 1$.

One can see in Fig. 6 a nonlinear increase in the time T_h with increasing the substrate concentration S_0. The time T_h is particularly high at low values of the diffusion module σ,

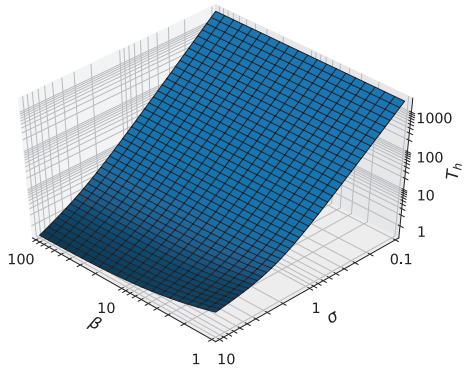

Figure 5. The dimensionless holding time T_h vs. the diffusion module σ and Biot number β at the dimensionless concentration $S_0 = 1$.

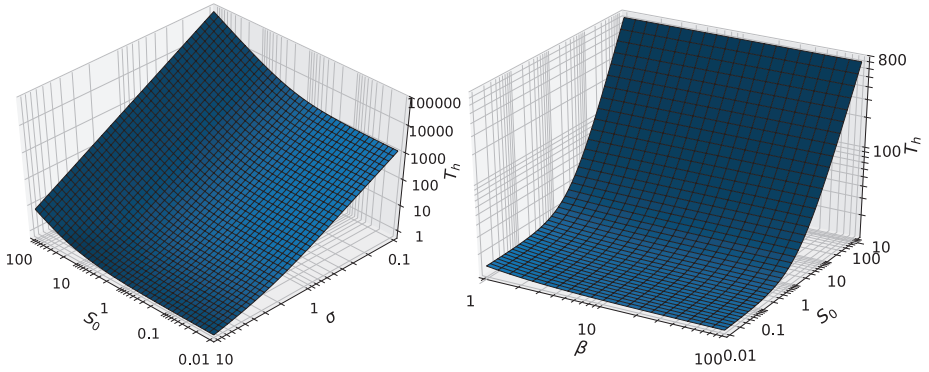

Figure 6. The dimensionless holding time T_h vs. the dimensionless concentration S_0 changing the diffusion module σ at the Biot number $\beta = 10$ (a) and changing the Biot number β at $\sigma = 1$ (b).

i.e. when the enzyme kinetics controls the MR action. So, the increasing MR effectiveness by the decreasing internal diffusion limitation (decreasing σ) as well as by increasing the substrate concentration is restricted when a short processing time is of crucial importance. The impact of the external diffusion resistance (β) on the time T_h is rather slight.

The complex nature of bioprocesses and microreactors involves consideration of the simultaneous optimization of several objectives some of which are conflicting, i.e. if one of them is improved, the others get worse [32]. The multi-objective optimization together with the multi-dimensional visualization can be used for finding a certain number of trade-off solutions and making decisions when designing microbioreactors [10, 28].

Very recently, when analyzing the stirred catalytic basket bioreactor for the production of bioethanol, it was observed that the time of the glucose consumption increases by increasing the glucose concentration in the bioreactor medium [25]. It was also observed that the time for consumption of glucose decreases with increase in stirrer speed.

Particularly, when using stirrer speed of 200 rpm and free cells as catalysts, the glucose consumption time was nearly 20 h, while at 500 rpm, the consumption time was about two times less [25]. Since the thickness of the Nernst diffusion layer for a flat surface decreases about $\sqrt{2.5}$ times when the stirrer speed increases 2.5 times and the radius of free cells is relatively small, the Biot number β then decreases about $\sqrt{2.5} \approx 1.6$ [11]. One can see in Fig. 5 similar decrease (about 2 times) in the holding time T_h when decreasing the Biot number in 1.6 times for small values of β. Figure 6 shows that the time T_h increases with increasing the substrate concentration as it was observed in [25].

Figure 6 shows how the MR holding time changes when the enzyme kinetics changes from first-order ($S_0 \ll 1$) through Michaelis–Menten to zero-order ($S_0 \gg 1$) kinetics.

6 Conclusions

The two-compartment mathematical model (2)–(9) and the corresponding dimensionless model (10)–(13) of a porous spherical microbioreactor acting in the continuous flow can be successfully used to investigate the dependence of the internal and external diffusion limitations on the bioreactor effectiveness and the process duration as well as to optimize the MR configuration (Fig. 1).

Approximate analytic solutions (31)–(34) of the nonlinear initial boundary value problem, obtained by the homotopy perturbation method (HPM), are of satisfactory accuracy when the enzyme kinetics controls the MR action, i.e. when $\sigma < 1$. Since MR designers usually seek for bioreactors acting in the reaction-limited regime, the approximate analytic solutions have a practical value.

The overall effectiveness factor η_o of MR monotonously increases with increasing the substrate concentration (S_0) as well as by decreasing the diffusion module σ. The effectiveness can be also but slightly increased by increasing the Biot number β (Figs. 3 and 4).

Increasing the MR effectiveness by decreasing the internal diffusion limitation (decreasing σ) as well as by increasing the substrate concentration (S_0) is restricted when a short processing time is of crucial importance (Figs. 5 and 6). Therefore, the multi-objective optimization together with the multi-dimensional visualization could be used for finding the trade-off solutions and making decisions when designing microbioreactors.

References

1. A.E. AL-Muftah, I.M. Abu-Reesh, Effects of simultaneous internal and external mass transfer and product inhibition on immobilized enzyme-catalyzed reactor, *Biochem. Eng. J.*, **27**(2):167–178, 2005.
2. M. Al-Shannag, Z. Al-Qodah, J. Herrero, J.A.C. Humphrey, F. Giralt, Using a wall-driven flow to reduce the external mass-transfer resistance of a bio-reaction system, *Biochem. Eng. J.*, **38**(3):554–565, 2008.
3. I. Andrés, *Enzyme Biocatalysis: Principles and Applications*, Springer, Dordrecht, 2008.

4. R. Aris, *Mathematical Modeling: A Chemical Engineer's Perspective*, Academic Press, London, 1999.
5. E. Babolian, A. Azizi, J. Saeidian, Some notes on using the homotopy perturbation method for solving time-dependent differential equations, *Math. Comput. Modelling*, **50**(1-2):213–224, 2009.
6. R. Bailey, F. Jones, B. Fisher, B. Elmore, Enhancing design of immobilized enzymatic microbioreactors using computational simulation, *Appl. Biochem. Biotechnol.*, **122**(1–3):639–652, 2005.
7. R. Baronas, F. Ivanauskas, J. Kulys, Modelling a biosensor based on the heterogeneous microreactor, *J. Math. Chem.*, **25**(2–3):245–252, 1999.
8. R. Baronas, F. Ivanauskas, J. Kulys, Mathematical modeling of biosensors based on an array of enzyme microreactors, *Sensors*, **6**(4):453–465, 2006.
9. R. Baronas, F. Ivanauskas, J. Kulys, *Mathematical Modeling of Biosensors*, Springer, Dordrecht, 2010.
10. R. Baronas, A. Žilinskas, L. Litvinas, Optimal design of amperometric biosensors applying multi-objective optimization and decision visualization, *Electrochim. Acta*, **211**:586–594, 2016.
11. P.N. Bartlett, *Bioelectrochemistry: Fundamentals, Experimental Techniques and Applications*, John Wiley & Sons, Chichester, UK, 2008.
12. L.A. Belfiore, *Transport Phenomena for Chemical Reactor Design*, John Wiley & Sons, Hoboken, NJ, 2003.
13. C.M. Bidabehere, J.R. García, U. Sedran, Transient effectiveness factor in porous catalyst particles. application to kinetic studies with batch reactors, *Chem. Eng. Res. Des.*, **118**:41–50, 2017.
14. D. Britz, R. Baronas, E. Gaidamauskaitė, F. Ivanauskas, Further comparisons of finite difference schemes for computational modelling of biosensors, *Nonlinear Anal. Model. Control*, **14**(4):419–433, 2009.
15. D. Britz, J. Strutwolf, *Digital Simulation in Electrochemistry,* 4th ed., Monographs in Electrochemistry, Springer, Cham, 2016.
16. D. Cascaval, A.I. Galaction, R. Rotaru, Effect of glucose internal diffusion on alcoholic fermentation in a stationary basket bioreactor with immobilized yeast cells, *Rom. Biotech. Lett.*, **16**(3):6200–6208, 2011.
17. L. Coche-Guerente, P. Labbé, V. Mengeaud, Amplification of amperometric biosensor responses by electrochemical substrate recycling. 3. Theoretical and experimental study of the phenol-polyphenol oxidase system immobilized in laponite hydrogels and layer-by-layer self-assembled structures, *Anal. Chem.*, **73**(14):3206–3218, 2001.
18. M.E. Davis, R.J. Davis, *Fundamentals of Chemical Reaction Engineering*, McGraw-Hill, New York, 2003.
19. D.D. Do, P.F. Greenfield, The concept of an effectiveness factor for reaction problems involving catalyst deactivation, *Chem. Eng. J.*, **27**(2):99–105, 1983.
20. P.M. Doran, *Bioprocess Engineering Principles,* 2nd ed., Academic Press, Waltham, MA, 2013.

21. D.A. Edwards, B. Goldstein, D.S. Cohen, Transport effects on surface-volume biological reactions, *J. Math. Biol.*, **39**(6):533–561, 1999.

22. D. Fink, T. Na, J.S. Schultz, Effectiveness factor calculations for immobilized enzyme catalysts, *Biotechnol. Bioeng.*, **15**(2):879–888, 1973.

23. R. Harriott, *Chemical Reactor Design*, Marcel Dekker, New York, 2003.

24. J.H. He, Homotopy perturbation technique, *Comput. Methods Appl. Mech. Eng.*, **178**(3–4):257–262, 1999.

25. A. Hussain, M. Kangwa, M. Fernandez-Lahore, Comparative analysis of stirred catalytic basket bio-reactor for the production of bio-ethanol using free and immobilized Saccharomyces cerevisiae cells, *AMB Express*, **7**(1):158, 2017.

26. J. Iqbal, S. Iqbala, C.E. Müller, Advances in immobilized enzyme microbioreactors in capillary electrophoresis, *Analyst*, **138**(11):3104–3116, 2013.

27. R. Kandiyoti, *Fundamentals of Reaction Engineering*, Ventus Publishing, Frederiksberg, 2009.

28. T. Keßler, F. Logist, M. Mangold, Bi-objective optimization of dynamic systems by continuation methods, *Comput. Chem. Eng.*, **98**:89–99, 2017.

29. O.M. Kirthiga, L. Rajendran, Approximate analytical solution for non-linear reaction diffusion equations in a mono-enzymatic biosensor involving Michaelis–Menten kinetics, *J. Electroanal. Chem.*, **751**:119–127, 2015.

30. A. Konti, D. Mamma, D.G. Hatzinikolaou, D. Kekos, 3-Chloro-1,2-propanediol biodegradation by Ca-alginate immobilized pseudomonas putida DSM 437 cells applying different processes: Mass transfer effects, *Bioproc. Biosyst. Eng.*, **39**(10):1597–1609, 2016.

31. J. Kulys, The development of new analytical systems based on biocatalysts, *Anal. Lett.*, **14**(6): 377–397, 1981.

32. M. Kunze, C. Lattermann, S. Diederichs, W. Kroutil, J. Büchs, Minireactor-based high-throughput temperature profiling for the optimization of microbial and enzymatic processes, *J. Biol. Eng.*, **8**:22, 2014.

33. H. Liu, X. Qian, Z. Du, P. Huang, Z. Liu, Thermal explosion model and calculation of sphere fireworks and crackers, *J. Therm. Anal. Calorim.*, **110**(3):1029–1036, 2012.

34. E. Nagy, J. Dudás, R. Mazzei, E. Drioli, L. Giorno, Description of the diffusive-convective mass transport in a hollow-fiber biphasic biocatalytic membrane reactor, *J. Membr. Sci.*, **482**: 144–157, 2015.

35. S. Petronis, M. Stangegaard, C.B.V. Christensen, M. Dufva, Transparent polymeric cell culture chip with integrated temperature control and uniform media perfusion, *Biotechniques*, **40**(3):368–376, 2006.

36. W.H. Press, S.A. Teukolsky, W.T. Vetterling, B.P. Flannery, *Numerical Recipes: The Art of Scientific Computing,* 3rd ed., Cambridge Univ. Press, Cambridge, 2007.

37. L. Rajendran, S. Anitha, Reply to "Comments on analytical solution of amperometric enzymatic reactions based on Homotopy perturbation method", by Ji-Huan He, Lu-Feng Mo [Electrochim. Acta (2013)], *Electrochim. Acta*, **102**:474–476, 2013.

38. U. Rinas, H. El-Enshasy, M. Emmler, A. Hille, D.C. Hempel, H. Horn, Model-based prediction of substrate conversion and protein synthesis and excretion in recombinant Aspergillus niger biopellets, *Chem. Eng. Sci.*, **60**(10):2729–2739, 2005.

39. J. Saranya, L. Rajendran, L. Wang, C. Fernandez, A new mathematical modelling using Homotopy perturbation method to solve nonlinear equations in enzymatic glucose fuel cells, *Chem. Phys. Let.*, **662**:317–326, 2016.

40. D. Schäpper, M.N.H.Z. Alam, N. Szita, A.E. Lantz, K.V. Gernaey, Application of microbioreactors in fermentation process development: a review, *Anal. Bioanal. Chem.*, **395**(3):679–695, 2009.

41. T. Schulmeister, Mathematical modelling of the dynamic behaviour of amperometric enzyme electrodes, *Select. Electr. Rev.*, **12**:203–260, 1990.

42. N.V. Torres, Application of the transition time of metabolic systems as a criterion for optimization of metabolic processes, *Biotechnol. Bioeng.*, **44**(3):291–296, 1994.

43. F.J. Valdés-Parada, J. Alvarez-Ramirez, J.A. Ochoa-Tapia, Analysis of mass transport and reaction problems using Green's functions, *Rev. Mex. Ing. Quim.*, **6**(3):283–294, 2007.

44. M. Velkovsky, R. Snider, D.E. Cliffel, J.P. Wikswo, Modeling the measurements of cellular fluxes in microbioreactor devices using thin enzyme electrodes, *J. Math. Chem.*, **49**(1):251–275, 2011.

45. J. Villadsen, J. Nielsen, G. Lidén, *Bioreaction Engineering Principles,* 3rd ed., Monographs in Electrochemistry, Springer, New York, 2011.

46. H.J. Vos, P.J. Heederik, J.J.M. Potters, K.Ch.A.M. Luyben, Effectiveness factor for spherical biofilm catalysts, *Bioprocess Eng.*, **5**(2):63–72, 1990.